Study on hydrate formation and gas selectivity in the presence of a kinetic hydrate inhibitor

ABSTRACT

This study investigated the effects of three process parameters—stirrer speed, salinity, and cooling rate—on the performance of a Kinetic Hydrate Inhibitor (KHI) in inhibiting sour gas hydrate formation and influencing the gas selectivity of hydrogen sulfide and carbon dioxide during this process.

The findings demonstrated that (1) the performance of the KHI improved significantly in the saline compared to the deionized water system, (2) Increasing the stirrer speed negatively impacted the performance of the KHI, which ultimately reduced the limiting effect of mass transfer between the two phases of gas and water, (3) Lowering the cooling rate decreased KHI performance by shortening nucleation and increasing hydrate growth.

Moreover, It was observed that the H_2S and CO_2 (acid gases) percentages concentrated in the gas phase after hydrate formation with KHI compared to its absence. This suggests that while KHI did not prevent hydrate formation, the risk of corrosion may increase due to the higher quantities of acid gases.

KEYWORDS: Sour gas hydrate formation, Gas selectivity, Kinetic hydrate inhibitor, Cooling rate, Stirrer speed, Salinity.

1. INTRODUCTION

Gas hydrate formation represents a significant operational challenge in oil and gas production systems, posing a major risk to stable hydrocarbon flow [1]. These ice-like crystalline solids, composed of water molecules forming cage-like structures that entrap low molecular weight gases, can rapidly nucleate and accumulate within pipelines and processing facilities under favorable high-pressure and low-temperature conditions [2]. Such blockages can lead to severe flow assurance problems, resulting in substantial production losses, costly remediation efforts, and increased safety and environmental risks, particularly when handling sour gas streams containing toxic hydrogen sulfide (H_2S) and corrosive carbon dioxide (CO_2) [3]. To mitigate this threat, the industry increasingly employs Kinetic Hydrate Inhibitors (KHIs), a class of chemical additives distinct from thermodynamic inhibitors. While the latter (e.g., methanol, monoethylene glycol) shift hydrate equilibrium conditions, KHIs function by adsorbing onto the surface of nascent hydrate crystals or critical clusters, thereby delaying the nucleation and subsequent growth phase for a duration sufficient to transport the fluid beyond the hydrate-prone region [4]. The effectiveness of a KHI is primarily evaluated by its ability to extend the induction time, defined as the stochastic period from the establishment of hydrate-forming conditions to the detectable onset of crystallization [5]. However, KHI performance is not intrinsic and is profoundly influenced by the system's specific operational and thermodynamic parameters, creating a complex optimization challenge [6]. This optimization is particularly critical in the context of sour gas systems and for the emerging technology of Hydrate-Based Gas Separation (HBGS). For sour gas, the acidic components H_2S and CO_2 exhibit a higher affinity for hydrate cages compared to methane (CH_4) under certain conditions, altering phase equilibria and kinetics [7]. In HBGS, this selectivity is intentionally exploited to separate CO_2 or H_2S from flue gas or natural gas streams by promoting controlled hydrate formation [8]. Here, the role of a KHI is paradoxical yet vital; it may be used to fine-tune the growth rate, preventing rapid, agglomerative plugging while allowing selective encapsulation for separation. Therefore, a comprehensive understanding of how key parameters interact with KHIs to govern hydrate kinetics is essential for both flow assurance and process design [9]. A primary parameter is agitation or stirring speed, which directly governs mass and heat transfer by influencing the gas-liquid interfacial area, bubble/droplet size distribution, and system homogeneity. Enhanced agitation typically increases the rate of gas dissolution into the aqueous phase, a critical step for hydrate formation. Research by Li et al. demonstrated an 80-fold increase in the mass transfer coefficient for sour gas hydrate formation when agitation was increased from 450 to 800 rpm [10]. Similarly, Qureshi and Atilhan

have studied the impact of stirring in high-pressure systems, highlighting its critical role in formation kinetics [11]. The cooling rate and degree of subcooling ($\Delta T = T_{equilibrium} - T_{operating}$) provide the thermodynamic driving force. A higher subcooling accelerates growth but, counterintuitively, can increase the stochasticity and average length of the nucleation induction period [12]. Furthermore, studies on hydrate film formation, such as those for CO_2, show additive and interfacial effects are critical at this stage [13]. This nonlinear relationship necessitates precise thermal management. The presence of salinity (e.g., NaCl, $CaCl_2$) introduces multifaceted effects. Salts act as thermodynamic inhibitors, depressing the hydrate equilibrium temperature [14]. During hydrate growth, salt is excluded from the crystal lattice, leading to a concentrated brine layer at the hydrate-water interface. This increases local subcooling initially but then rapidly reduces the local driving force, potentially quenching growth more quickly than in pure water systems [15]. Research on methane hydrates in synthetic seawater has quantified these dissociation behaviors [16]. Furthermore, salinity can affect KHI solubility and adsorption efficiency [17], and it can alter the composition of the hydrate phase, reducing the uptake of H_2S, which impacts separation selectivity in HBGS [18]. The stability of hydrates in saline environments also has implications for long-term applications like CO_2 storage [19]. Other vital operational parameters for process optimization include the gas-to-water ratio (GWR), which affects conversion yield and the multiphase flow regime; the water-to-oil (or condensate) ratio, as the presence of a hydrocarbon liquid phase can solubilize hydrate formers and alter the locus of hydrate formation (e.g., at the water-oil interface or within water droplets) [20]; absolute system pressure and temperature, which define the operational point relative to the hydrate equilibrium curve [21]; and the precise sour gas composition ($H_2S/CO_2/CH_4$ ratios), which dictates the equilibrium conditions and relative occupancies in the hydrate cages [22]. The performance evaluation of a KHI in such a complex milieu requires a comparative analysis against an uninhibited control test, measuring metrics like induction time, initial growth rate, final gas consumption, and hydrate morphology. Studies by Perfeldt et al. and Park et al. demonstrate that the efficacy of an inhibitor hinges on its ability to suppress the growth rate and prolong the induction time under the optimized set of these operational parameters [23, 24].

This study investigated the effects of three process parameters—stirrer speed, salinity, and cooling rate—on the performance of a Kinetic Hydrate Inhibitor (KHI) in inhibiting sour gas hydrate formation. Additionally, it examined the impact of KHI on gas phase composition post-hydrate formation in relation to flow assurance in the pipeline.

2. EXPERIMENTAL SECTION

2.1. MATERIALS

The synthesis sour gas was provided by Arkan Gas Co. with the composition given in Table 1. The liquid gas condensate used in the tests were sampled from a field pipeline. Brine was prepared based on 10wt% sodium chloride using distilled water (DW) in preparing solutions. A commercial kinetic inhibitor, called here KHI, were used in the tests.

Table 1. Synthesis sour gas composition

Component	Mol%
CO_2	2.460
H_2S	0.090
CH_4	86.470
C_2H_6	4.910
C_3H_8	1.580
Total	100.000

2.2. APPARATUS

A 700-ml stainless steel high-pressure tank with a maximum operational pressure of 150 bar was used. A magnetic-drive stirrer and an electric motor equip the reactor for proper mixing. Reactor pressure over time is measured by a pressure sensor with an accuracy of 0.2 bar, and the reactor temperature is measured by a temperature sensor with an accuracy of 0.1 °C and a working range of -20 to 100 °C. An adjustable water bath controls the reactor temperature. Changes in reactor pressure and temperature over time are recorded by an in-house software.

2.3. METHOD

This test method, based on simulating the temperature, pressure, and phase composition conditions of an offshore pipeline, is taken from an internal manual of a gas production company active in the gas field in southern Iran. The volumetric ratio of gas to liquid is considered 60 to 40, with a condensate-to-water ratio of 6 to 1 based on a real field ratio. When the reactor temperature stabilizes, the data collecting software is activated. The initial temperature and pressure is considered 20 °C and 122 bar, respectively. The reactor temperature is reduced from 20 to 12°C at a rate of 5°C/h in accordance with a temperature program. Hydrate formation delay time and pressure drop respect to hydrate growth were measured.

3. RESULTS AND DISCUSSION

In an internal manual for a gas production company in southern Iran, stirrer speed (500 rpm), no salinity, and a cooling rate of 5 °C/h were set to simulate offshore pipeline conditions. The study analyzed the sensitivity of hydrate formation to these parameters and their impact on KHI performance based on delay time and pressure drop. Figure 2 represents typically the temperature and pressure profiles of hydrate formation for the blank test in the presence of distilled water and condensate

A simultaneous peak in temperature alongside a pressure drop, indicative of hydrate formation, is illustrated in Figure 2. The delay time, which is the duration taken to observe this sign of hydrate formation, was noted after the temperature reached 12 °C. The corresponding pressure drop and delay time for various process conditions are provided in Table 2.

In Table 2, the distilled water (DW) system in run 1 and the brine system in run 7 showed similar hydrate formation results, with both having a 0.5-hour delay time and pressure drops of 6.8 bar for DW and 6.5 bar for brine. However, salinity significantly affected the kinetic hydrate inhibitor (KHI) performance. In the DW system, KHI in run 3 delayed hydrate formation from 0.5 to 5.0 hours and reduced the pressure drop from 6.8 to 2.5 bar. In the brine system, KHI in run 8 delayed formation by over 48 hours compared to the blank test in run 7, indicating that KHI effectiveness is greatly improved in saline conditions. This indicates that the KHI is more effective in preventing hydrate formation when salts are present, likely due to interactions that enhance its performance in these conditions.

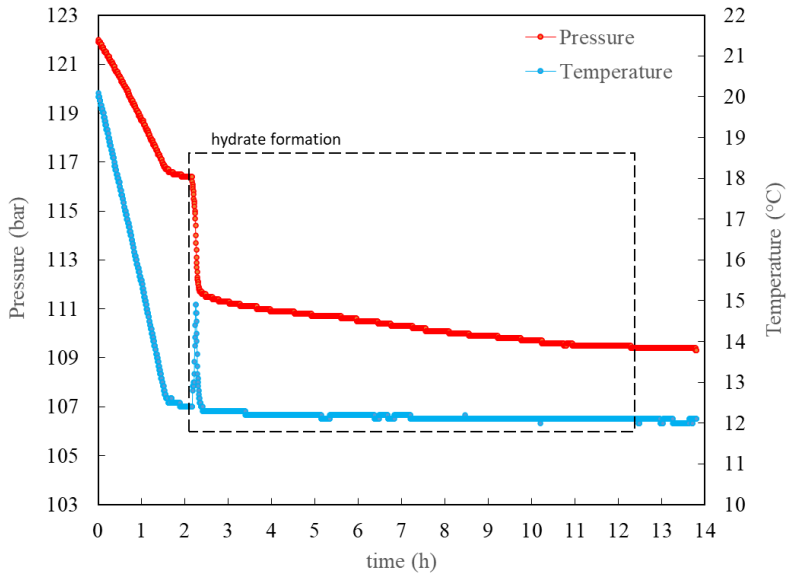

Figure 2. Temperature and pressure profiles of the blank hydrate formation test in the presence of distilled water and condensate (the blue line: temperature and the red line: pressure profile)

Examining the effect of fluid mixing rate on the performance of the KHI, it was found that at a stirring speed of 300 RPM (run 2), no hydrates formed even after 48 hours. However, when the stirring speed was increased to 500 RPM, the delay time for hydrate formation decreased to just 5 hours (run 3). In the subsequent stage, when stirring speed was doubled to 1000 RPM, the effectiveness of the KHI diminished significantly, resulting in a reduced inhibition time of only 1.5 hours (run 4). Fluid mixing can significantly influence mass transfer in the heterogeneous process of hydrate formation. As observed, at a stirring speed of 300 rpm, the mixing may act as a limiting factor. However, when the stirring speed is increased to 500 or 1000 rpm, the performance of the kinetic hydrate inhibitor (KHI) in delaying hydrate formation appears to weaken.

At the cooling rates of 1, 5, and 10 °C/h (run 5, 3 and 6), the hydrate formation delay times were 1.5, 5, and 6.5 hours, while the associated pressure drops were 5, 2.5, and 2.5 bar. When the cooling rate was comparatively low (1 °C/h in comparison to 5 and 10 °C/h), it had a severe adverse effect on the performance of the KHI. This was evidenced by a reduction in the delay time of hydrate formation, which shortens the nucleation process, as well as an increase in the pressure drop associated with hydrate formation, leading to enhanced hydrate crystal growth.

When hydrate formation occurs from a gas mixture, different molecules exhibit varying selectivity in entering the hydrate structure. As a result, the gas composition in equilibrium with the solid hydrate at the end of the growth process differs from the initial gas composition. the presence of a Kinetic Hydrate Inhibitor (KHI) influence gas molecule selectivity in entering the hydrate structure and the composition of the remaining gas phase compared to when KHI is absent, was investigated.

Table 2. The results summery of hydrate formation tests

Run	KHI	Water phase	Hydrocarbone phase	Stirrer speed (rpm)	Cooling rate (^{o}C/h)	Delay time (h)	Pressure drop (bar)
1	×	DW	Condensate	500	5	0.5	6.8
2	✓	DW	Condensate	300	5	48<	-
3	✓	DW	Condensate	500	5	5.0	2.5
4	✓	DW	Condensate	1000	5	1.5	3.0
5	✓	DW	Condensate	500	1	1.5	5.0
6	✓	DW	Condensate	500	10	6.5	2.5
7	×	Brine	Condensate	500	5	0.5	6.5
8	✓	Brine	Condensate	500	5	48<	-

Although acid gas molecules (H2S and CO2) are believed to be more likely to enter the hydrate structure than larger compounds, it was observed that the presence of a Kinetic Hydrate Inhibitor (KHI) during run 3 decreased the tendency of acid gas molecules to enter the hydrate structure. As a result, a higher composition of acid gas molecules was noted in Table 3 when compared to the absence of KHI in run 1.

Table 3. Sour gas composition after hydrate formation

component	In the absence of KHI Mol%	In the presence of KHI Mol%
CO_2	0.006	0.022
H_2S	0.000	0.001
CH_4	0.946	0.922
C_2H_6	0.035	0.043
C_3H_8	0.012	0.012
Total	100.000	100.000

4. CONCLUSION

The impact of three parameters—stirrer speed, salinity, and cooling rate—on the performance of the Kinetic Hydrate Inhibitor (KHI) in controlling hydrate formation was investigated through laboratory tests aimed at simulating the conditions of offshore pipelines.

While the behavior of the fluid in the absence of the hydrate inhibitor was similar for both the deionized water (DW) and saline systems, the performance of the kinetic hydrate inhibitor (KHI) improved significantly in the saline system.

A low cooling rate (1 °C/h compared to 5 and 10 °C/h) severely impacted KHI performance by reducing the delay time for hydrate formation, thus shortening nucleation, and increasing the pressure drop during hydrate formation, leading to greater crystal growth.

Overall, increasing the stirrer speed led to enhanced fluid mixing and improved contact between the water and gas phases, negatively impacting the performance of the kinetic inhibitor for hydrate.

Finally, it was observed that the presence of KHI reduced the tendency of acid gas molecules to enter the hydrate structure, resulting in a higher acid gas composition after hydrate formation, which could increase corrosion risk subsequently.

5. References

1. Sloan, E. D., & Koh, C. A. (2008). Clathrate Hydrates of Natural Gases* (3rd ed.). CRC Press, DOI:10.1201/9781420008494.

2. Carroll, J. J. (2014). Natural Gas Hydrates: A Guide for Engineers (3rd ed.). Gulf Professional Publishing. DOI: 10.1016/C2013-0-15367-1.

3. Kelland, M. A. (2006). History of the Development of Low Dosage Hydrate Inhibitors. Energy & Fuels, 20(3), 825–847, DOI:10.1021/ef050427x.

4. Zarringhalam, M., Talaghat, M. R., & Esmaeilzadeh, F. (2012). Experimental investigation of induction time for double gas hydrate formation in the simultaneous presence of the PVP and l-Tyrosine as kinetic inhibitors in a mini flow loop apparatus. Journal of Natural Gas Science and Engineering, 9, 125–131, DOI:10.1016/j.jngse.2014.05.010.

5. Brandel, C. and Horst, H. (2015). Measuring induction times and crystal nucleation rates. Faraday Discuss., 179, 199-214, DOI: 10.1039/C4FD00230J

6. Babu, P., Linga, P., Kumar, R., & Englezos, P. (2015). A review of the hydrate based gas separation (HBGS) process for carbon dioxide pre-combustion capture. Energy, 85, 261–279, DOI: 10.1016/j.energy.2015.03.103.

7. Anderson, R., & Tohidi, B. (2011). The role of interfacial phenomena in the kinetics of gas hydrate formation. Chemical Engineering Science, 66(23), ٥٧٥٩–٥٧٦٨. DOI: 10.1016/j.ces.2011.07.037

8. Li, X., Wu, H., & Wang, Y. (2018). Enhancement of mass transfer for sour gas hydrate formation in a stirred reactor. Energy & Fuels, 32(5), 5781–5790. DOI: 10.1021/acs.energyfuels.8b00600

9. Qureshi, M. F., & Atilhan, M. (2017). The Effect of Stirring on Gas Hydrate Formation in High Pressure Reactor Systems. AIChE Spring Meeting and Global Congress on Process Safety. Paper ID: 489973

10. Uchida, T., Ebinuma, T., Kawabata, J. I., & Narita, H. (2002). CO_2 hydrate film formation at the boundary between CO_2 and water: effects of temperature, pressure and additives on the formation rate. Journal of Crystal Growth, 237-239, 383–387, DOI:10.1016/S0022-0248(01)01822-X.

11. Masoudi, R., Tohidi, B., Danesh, A., & Todd, A. C. (2004). A new approach in modelling phase equilibria and gas solubility in electrolyte solutions and its applications to gas hydrates. Fluid Phase Equilibria, 215(2), 163–174, DOI: 10.1016/j.fluid.2003.08.009.

12. ZareNezhad, B., & Aminian, A. (2013). Predicting the effects of salt and inhibitor on the hydrate induction time. Chemical Engineering Research and Design, 91(6), 1056–1062., DOI: 10.1016/j.cherd.2012.11.002.

13. Saw, V. K., Udayabhanu, G., Mandal, A., Laik, S., & Sangwai, J. S. (2012). Methane hydrate formation and dissociation in synthetic seawater. Journal of Natural Gas Chemistry, 21(6), 625–632, DOI: 10.1016/S1003-9953(11)60411-8.

14. Husebø, J., Ersland, G., Graue, A., & Kvamme, B. (2009). Effects of salinity on hydrate stability and implications for storage of CO_2 in natural gas hydrate reservoirs. Energy Procedia, 1(1), 3731–3738, DOI: 10.1016/j.egypro.2009.02.172.

15. Sun, Q., Chen, G., & Guo, X. (2019). Influence of water-to-oil ratio on hydrate formation and plugging in water-in-oil emulsions. AIChE Journal, 65(11), e16735. DOI: 10.1002/aic.16735.

16. Eslamimanesh, A., Mohammadi, A. H., & Richon, D. (2012). Phase equilibrium modeling of clathrate hydrates of methane, carbon dioxide, nitrogen, and hydrogen sulfide. Chemical Engineering Science, 81, 319–328. DOI: 10.1016/j.ces.2012.06.012.

17. Mohammadi, A. H., Richon, D., & Tohidi, B. (2013). Predicting the hydrate stability zones of sour natural gases using a thermodynamic model. Industrial & Engineering Chemistry Research, 52(35), 12394–12401. DOI: 10.1021/ie401344z.

18. Karimi, R., Varaminian, F., & Izadpanah, A. A. (2013). Investigating the effect of various factors on the kinetics of ethane hydrate formation in the presence of surfactants. The Second National Gas Hydrate Conference of Iran. COI: HYDRATE02_028.

19. Hu, Z., Zhang, J., & Chen, G. (2017). Inhibition performance of kinetic hydrate inhibitors in the presence of salts and monoethylene glycol for sour gas fields. Journal of Chemical & Engineering Data, 62(1), 244–251. DOI: 10.1021/acs.jced.6b00688.

20. Naeiji, P., Varaminian, F., & Arjomandi, A. (2014). Kinetic study of hydrate formation in the presence of kinetic inhibitors. Journal of Molecular Liquids, 194, 143–149. DOI: 10.1016/j.molliq.2014.01.030.

21. Hassanpouryouzband, A., Joonaki, E., Vasheghani Farahani, M., Takeya, S., Ruppel, C., Yang, J., ... & Tohidi, B. (2020). Gas hydrates in sustainable chemistry. Chemical Society Reviews, 49(15), 5225–5309, DOI: 10.1039/c8cs00989a.

22. Bavoh, C. B., Lal, B., & Osei, H. (2019). A review on the role of amino acids in gas hydrate inhibition. Journal of Molecular Liquids, 296, 111850, DOI: 10.1016/j.jngse.2019.01.020.

23. Perfeldt, C. M., Chua, P. C., & Daraboina, N. (2014). Inhibition of methane hydrate formation by a glycol-based kinetic inhibitor. Energy & Fuels, 28(11), 7079–7086. DOI: 10.1021/ef5018698.

24. Park, J., & Kim, H. (2019). Effect of hydrate formation conditions on the separation efficiency of CO_2 from fuel gas mixture via hydrate-based process. Chemical Engineering Journal, 369, 686–695. DOI: `10.1016/j.cej.2019.03.111.